

Fabrication of two-dimensional Au@FePt core-shell nanoparticle arrays by photochemical metal deposition

Thomas Härtling,^{1,a)} Tino Uhlig,¹ Axel Seidenstücker,² Nadja C. Bigall,³ Phillip Olk,¹ Ulf Wiedwald,² Luyang Han,² Alexander Eychemüller,⁴ Alfred Plettl,² Paul Ziemann,² and Lukas M. Eng¹

¹*Institut für Angewandte Photophysik, Technische Universität Dresden, 01062 Dresden, Germany*

²*Institut für Festkörperphysik, Universität Ulm, 89069 Ulm, Germany*

³*Istituto Italiano di Tecnologia (IIT), Via Morego 30, I-16163 Genova, Italy*

⁴*Physikalische Chemie und Elektrochemie, Technische Universität Dresden, 01062 Dresden, Germany*

(Received 19 February 2010; accepted 14 April 2010; published online 6 May 2010)

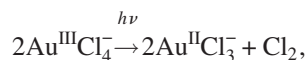
In this report, we experimentally demonstrate that single platinum nanoparticles exhibit the necessary catalytic activity for the optically induced reduction of H[AuCl₄] complexes to elemental gold. This finding is exploited for the parallel Au encapsulation of FePt nanoparticles arranged in a self-assembled two-dimensional array. Magnetic force microscopy reveals that the thin gold layer formed on the FePt particles leads to a strongly increased long-term stability of their magnetization under ambient conditions. © 2010 American Institute of Physics. [doi:10.1063/1.3425670]

Magnetic nanoparticles are promising nanoscale tools for the realization of high-density data storage media,^{1,2} sensing applications,³ medical imaging,^{4,5} and the fabrication of nanostructured materials.^{6–8} However, many magnetic materials in use tend to oxidize fast under ambient conditions and thereby lose the desired magnetic properties.⁹ Furthermore, surface functionalization of nanomagnets is difficult but vital to ensure biocompatibility or to provide specific molecular binding sites at the particle surface.^{10,11} To circumvent these problems, the fabrication of a thin gold shell around a magnetic particle core has been pursued during the past years. Several fabrication protocols for such core-shell-type nanoparticles in solution have been used with different success.^{12–14} Here, we report on a simple and reliable technique which extends Au shell fabrication to magnetic particles arranged in two-dimensional ordered arrays. The approach exploits the optically induced deposition of gold from a gold salt solution onto catalytically active nanoparticles and leads to the formation of a protective layer on the particle surface.

We at first provide an experimental proof that single Pt particles catalyze the photochemical reduction in H[AuCl₄] resulting in Au@Pt core-shell nanoparticles. Spherical Pt particles (average diameter 30 nm) were prepared in an aqueous solution according to a protocol we reported earlier.¹⁵ The particles were extracted from the solution by blow-drying a droplet on a clean cover glass. The sample was then mounted on an inverted optical microscope as described in detail in Ref. 16. The particles were embedded in a droplet of a 5 μM H[AuCl₄] solution. In order to avoid evaporation and to assure optimal light transmission, a chemically inert optical immersion liquid was chosen as the solvent (No. 1160, Cargille Laboratories). Au deposition was triggered by irradiation of single Pt particles with laser light (532 nm, 1 mW) focused to a diffraction-limited spot. For monitoring

the deposition process, the laser beam was blocked and the sample was illuminated with white light from a xenon arc lamp. The intensity of the white light was kept below 10 μW to ensure that no relevant amount of gold was deposited during white-light irradiation. Light scattered from a single particle was analyzed using a grating spectrometer and a cooled CCD camera in a confocal detection path.

Upon irradiation, AuCl₄[−] ions from the solution are reduced to elemental Au at the particle surface forming a thin Au shell. This shell exhibits a localized surface plasmon resonance which manifests itself as the peak emerging around 540 nm in the scattering spectrum shown in Fig. 1(a). In short, the chemical reaction proceeds as¹⁷



The first reaction step is triggered by photon absorption, while the second and the third steps are disproportionation reactions with the last reaction step requiring a catalyst.¹⁸ As the reduction in the gold complex takes place as part of a disproportionation, the solvent does not play any role in this reaction. Thus, identical experimental results were obtained when, e.g., water was used as the solvent. Furthermore, scanning electron microscopy (SEM) images verify that gold was deposited exclusively onto the seed particle, i.e., no traces of metal were observed on the substrate next to the particles (data not shown).¹⁹

We calculated the scattering spectrum of a single core-shell particle by means of the multiple-multipole (MMP) method.²⁰ For the dielectric function of Au the data of Johnson and Christy²¹ were used, and those of Weaver²² for Pt. In our model, a 30 nm Pt particle is covered with an Au shell of increasing thickness and homogeneously embedded in a dielectric material of $n=1.52$ representing the solvent. Presumably, no gold can be deposited in the region of contact between the particle and the substrate. We therefore considered the core and the shell to be noncentrosymmetric in

^{a)} Author to whom correspondence should be addressed. Electronic mail: thomas.haertling@izfp-d.fraunhofer.de. Present address: Fraunhofer Institute for Non-Destructive Testing, Maria-Reiche-Strasse 2, 01109 Dresden, Germany.

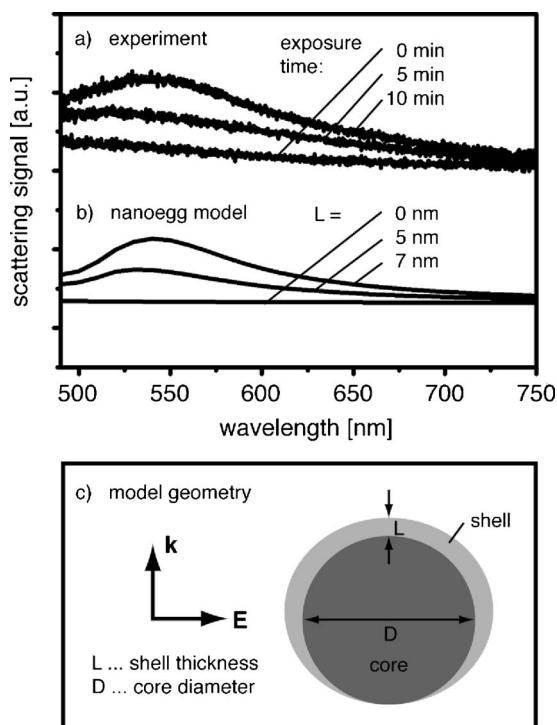


FIG. 1. (a) Experimentally determined scattering spectra during gold deposition onto a single Pt nanosphere (30 nm). (b) Calculated scattering spectra of Au@Pt particles. A gold layer of thickness L was assumed in the calculations performed according to the model geometry depicted in (c).

so-called nanoegg geometry as depicted in Fig. 1(c). On the upper particle hemisphere, the layer thickness was considered to be homogeneous. On the lower hemisphere, the layer thickness decreases to zero at the contact point between the substrate and the particle. Note that the substrate had the same permittivity as the immersion oil, and hence the surrounding medium was assumed to be homogeneous with $n = 1.52$. The simulations obtained with this model indeed reproduce the features of the experimental spectra, especially the growing peak around 540 nm. In sum, these experimental and theoretical findings demonstrate the catalytic activity of the Pt particle surface on the gold salt reduction and the formation of a gold shell around the Pt particles due to the site-selective deposition.

These results were exploited for the deposition of a gold shell on FePt particles arranged in two-dimensional arrays. Such arrays on glass (BK7) substrates were obtained by applying a micellar technique as described elsewhere.²³ The applied parameters led to an array of particles with an average diameter of 5 nm, self-assembled in a monolayer with a characteristic next-neighbor distance of about 45 nm. These 5 nm FePt nanoparticles show a surface enrichment of Pt after annealing at 650 °C for 60 min.⁹ Depending on the particle diameter, a thin Pt segregation layer in the order of 0.1–0.3 nm is formed and used here for site-selective Au deposition.²⁴

To this end, a HAuCl_4 solution of 5 mM concentration was prepared with the same solvent as used above. A 20 μl droplet of the solution formed a homogeneous liquid film on the $10 \times 5 \text{ mm}^2$ glass substrate with exception of the very edges only. The solution was irradiated homogeneously with the collimated beam of a Hg lamp for 3 min (Osram; spectral emission range between 350 and 450 nm; 10.2 m W cm^{-2}).

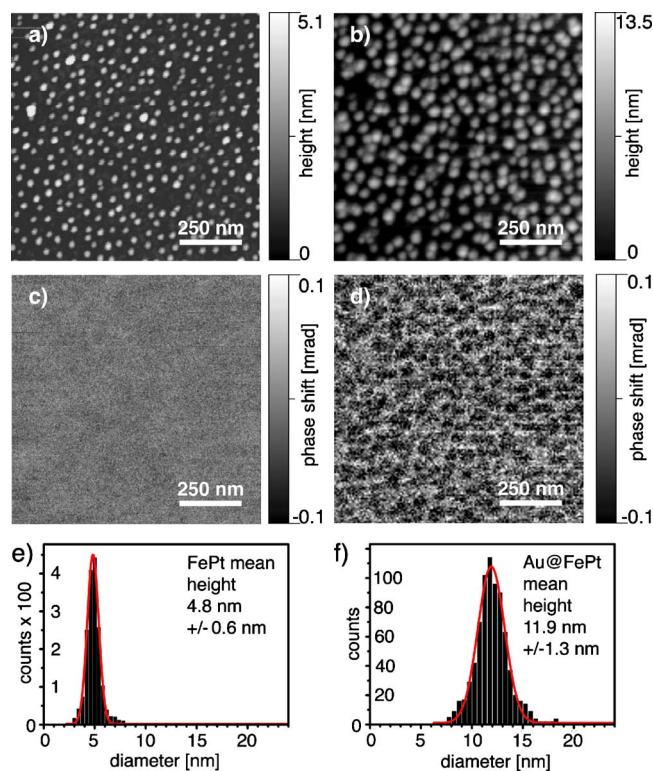


FIG. 2. (Color online) AFM topography images of as-prepared FePt particles (a) and gold-coated particles (b). [(c) and (d)] MFM phase shift images of the same locations as in (a) and (b), respectively, after exposure to air for 4 months. [(e) and (f)] Height distributions and mean diameters for the images shown in (a) and (b), respectively.

After irradiation, the solution remained on the substrate for additional 30 s. Then, it was removed in subsequent acetone and isopropyl alcohol baths.

Two different types of samples were fabricated. At first, freshly prepared FePt particles on glass substrates were covered with the gold salt solution directly after being locked out of the vacuum chamber. The exposure time to ambient conditions was approximately 10 min. After irradiation and rinsing, the sample was further exposed to ambient conditions for 4 months. A control sample of uncoated FePt particles processed under identical conditions except photochemical Au deposition served as a reference. After this storage time, the particle size and the size distribution of both samples were investigated by means of atomic force microscopy (AFM) (SmartSPM 1000 AFM setup, AIST-NT). Results are presented in Fig. 2, where panel (a) shows the topography of the uncoated FePt particles and (b) the gold-coated particles. The related height histograms are given in panels (e) and (f), respectively, and show an increase in particle height of 7 nm. Moreover, from the size histograms it is obvious that all particles were covered without fail. Despite the significant size increase in the particles, their lateral density is conserved, i.e., no additional particles were formed in between the FePt seed particles. This observation demonstrates the selectivity of the Au deposition as a consequence of the catalytic activity of the seeds.

Finally, we shortly address the degradation of magnetic properties for uncoated and Au-covered FePt nanoparticles. Magnetic force microscopy (MFM) measurements were carried out using an AFM with a magnetic probe (MagneticMulti75-G, Budget Sensors) in two-pass mode.

The investigations were conducted on the same day under identical conditions, i.e., with the identical magnetic tip and the same lift height of 35 nm. This lift height, compared to the particle height of 5 nm and 12 nm, respectively, assured that the signal from the second pass was not affected by topography cross talk. The results are presented in Figs. 2(c) and 2(d). A comparison of the purely magnetic contrast produced by the uncoated particles [Fig. 2(c)] and the gold-coated spheres [Fig. 2(d)] shows that the latter still exhibit magnetic contrast, while their uncoated pendants are invisible in the phase shift image. Thus, the Au coating of the FePt particles sizeably improves the long-term stability of their magnetic properties.

In conclusion, we demonstrated the optically induced deposition of a thin gold layer around Pt and FePt particles. To accomplish that, first the Au growth around Pt nanoparticles was proven by light scattering from single Pt nanoparticles. The light-induced Au layer deposition was then extended to the simultaneous growth of Au shells on many FePt nanoparticles arranged over macroscopic sample areas ($10 \times 5 \text{ mm}^2$) by exposure to a Hg vapor light source. As a result, the growth of a thin Au shell around the FePt particles was observed as determined by AFM height histograms. Finally, the magnetic long-term stability of Au-coated FePt particles was compared to that of uncoated reference particles by MFM. The coated particles still showed magnetic contrast after exposure to ambient conditions for 4 months, while the naked FePt nanoparticles had lost their magnetic properties completely. In future experiments, we will investigate the oxidation state of the FePt cores in order to quantify the protective effect of the gold shell.

The authors thank Paul Walther/Ulm University for providing SEM access. Funding by the SFB 569, Landesstiftung Baden-Württemberg, DFG Research Training Group "Nano- und Biotechniken für das Packaging elektronischer Systeme," by the European Union within the STREPs "PLEAS" and "PLAISIR," and FhG Internal Programs (Grant No. Attract 692271) is gratefully acknowledged.

- ¹S. Sun, *Adv. Mater.* **18**, 393 (2006).
- ²D. M. Newman, M. L. Wears, M. Jollie, and D. Choo, *Nanotechnology* **18**, 205301 (2007).
- ³A.-H. Lu, E. L. Salabas, and F. Schüth, *Angew. Chem. Int. Ed.* **46**, 1222 (2007).
- ⁴G. Reiss and A. Hütten, *Nature Mater.* **4**, 725 (2005).
- ⁵O. T. Bruns, H. Itrich, K. Peldschus, M. G. Kaul, U. I. Tromsdorf, J. Lauterwasser, M. S. Nikolic, B. Mollwitz, M. Merkel, N. C. Bigall, S. Sapra, R. Reimer, H. Hohenberg, H. Weller, A. Eychmüller, G. Adam, U. Beisiegel, and J. Heeren, *Nat. Nanotechnol.* **4**, 193 (2009).
- ⁶H. Liu, Y. M. Liu, T. Li, S. M. Wang, S. N. Zhu, and X. Zhang, *Phys. Status Solidi B* **246**, 1397 (2009).
- ⁷A. K. Sarychev, G. Shvets, and V. M. Shalaev, *Phys. Rev. E* **73**, 036609 (2006).
- ⁸B. Nandan, E. B. Gowd, N. C. Bigall, A. Eychmüller, P. Formanek, P. Simon, and M. Stamm, *Adv. Funct. Mater.* **19**, 2805 (2009).
- ⁹L. Han, U. Wiedwald, B. Kuerbanjiang, and P. Ziemann, *Nanotechnology* **20**, 285706 (2009).
- ¹⁰S. Sun, C. B. Murray, D. Weller, L. Folks, and A. Moser, *Science* **287**, 1989 (2000).
- ¹¹P. de la Presa, M. Multigner, M. P. Morales, T. Rueda, E. Fernandez-Pinel, and A. Hernando, *J. Magn. Magn. Mater.* **316**, e753 (2007).
- ¹²L. Wang, J. Luo, M. M. Maye, Q. Fan, Q. Rendeng, M. H. Engelhard, C. Wang, Y. Lin, and C.-J. Zhong, *J. Mater. Chem.* **15**, 1821 (2005).
- ¹³J. Zhang, M. Post, T. Veres, Z. J. Jakubek, J. Guan, D. Wang, F. Normandin, Y. Deslandes, and B. Simard, *J. Phys. Chem. B* **110**, 7122 (2006).
- ¹⁴Z. Xu, Y. Hou, and S. Sun, *J. Am. Chem. Soc.* **129**, 8698 (2007).
- ¹⁵N. C. Bigall, T. Härtling, M. Klose, P. Simon, L. M. Eng, and A. Eychmüller, *Nano Lett.* **8**, 4588 (2008).
- ¹⁶T. Härtling, Y. Alaverdyan, M. T. Wenzel, R. Kullock, M. Käll, and L. M. Eng, *J. Phys. Chem. C* **112**, 4920 (2008).
- ¹⁷E. Gachard, H. Remita, J. Khatouri, B. Keita, L. Nadjo, and J. Belloni, *New J. Chem.* **22**, 1257 (1998).
- ¹⁸T. Härtling, A. Seidenstücker, P. Olk, A. Plettl, P. Ziemann, and L. M. Eng, *Nanotechnology* **21**, 145309 (2010).
- ¹⁹Due to the limited resolution of the SEM and the small differences in electronic configuration between the involved metals, no material contrast between core and shell of the particles can be observed in these images.
- ²⁰C. Hafner, *Post-modern Electromagnetics: Using Intelligent Maxwell Solvers* (Wiley, New York, 1999).
- ²¹P. B. Johnson and R. W. Christy, *Phys. Rev. B* **6**, 4370 (1972).
- ²²J. H. Weaver, *Phys. Rev. B* **11**, 1416 (1975).
- ²³A. Ethirajan, U. Wiedwald, H. Boyen, B. Kern, L. Han, A. Klimmer, F. Weigl, G. Kästle, P. Ziemann, K. Fauth, J. Cai, R. J. Behm, A. Romanyuk, P. Oelhafen, P. Walther, J. Biskupek, and U. Kaiser, *Adv. Mater.* **19**, 406 (2007).
- ²⁴R. Wang, O. Dmitrieva, M. Farle, G. Dumpich, M. Acet, S. Mejia-Rosales, E. Perez-Tijerina, M. J. Yacaman, and C. Kisielowski, *J. Phys. Chem. C* **113**, 4395 (2009).